

1 A novel benzoxaborole works by targeting FabI in *Escherichia coli*

2

3 Soma Mandal¹ and Tanya Parish^{1,2*}

4

5

6 ¹Infectious Disease Research Institute, Seattle, WA, USA

7 ²Seattle Children's Research Institute, Seattle, WA, USA

8 * Corresponding author: tanya.parish@seattlechildrens.org

9

10

11

12

13 **Abstract**

14 To combat the looming crisis of antimicrobial-resistant infections, there is an urgent need for novel
15 antimicrobial discovery and drug target identification. The benzoxaborole series were previously
16 identified as inhibitors of mycobacterial growth. Here, we demonstrate that a benzoxaborole is also active
17 against the Gram negative bacterium, *Escherichia coli* in vitro. We isolated resistant mutants of *E. coli*
18 and subjected them to whole genome sequencing. We found mutations in the enoyl acyl carrier protein
19 FabI. Mutations mapped around the active center site located close to the co-factor binding site. This site
20 partially overlaps with the binding pocket of triclosan, a known FabI inhibitor. Similar to triclosan, the
21 interaction of the benzoxaborole with FabI was dependent on the co-factor NAD⁺. Identification of the
22 target of this compound in *E. coli* provides scope for further development and optimization of this series
23 for Gram negative pathogens.

24

25 **Introduction**

26 Antimicrobial resistance is a growing problem and at current rates of increase, it is estimated by the year
27 2050 ~10 million people will die due to infections caused by resistant bacteria (1). In order to tackle this
28 crisis, we need to identify and characterize novel scaffolds for development as new antimicrobial agents.
29 We previously identified AN11527, a benzoxaborole based compound as a potent inhibitor of
30 *Mycobacterium tuberculosis* growth (2). This is an attractive series, since it has good antibacterial activity
31 against extracellular and intracellular bacteria but lacks cytotoxicity. The target for this series is unknown,
32 although resistant mutants had single nucleotide polymorphisms in three genes (Rv1683 Rv3068c and
33 Rv0047c) (2). Rv0047c is involved in inositol metabolism, Rv3068c encodes a non-essential protein
34 involved in glucose metabolism (PgmA) and Rv1683 encodes a bifunctional protein involved in
35 triglyceride metabolism with both lipase and synthetase activity (3).

36

37 In this study we show that AN11527 is active against *Escherichia. coli*. We identified the cellular target
38 of AN11527 in *E. coli* as the enoyl-acyl carrier protein reductase FabI. We determined a potential binding
39 pocket for AN11527 which is located at the active center site and close to the cofactor binding site. We
40 also determined that the binding interactions of AN11527 partially overlaps with that of the NAD⁺-
41 dependent inhibitor Triclosan, but not that of the co-factor independent 4-hydroxy-2-pyridine compound
42 NITD-916.

43

44 **Materials and methods**

45 **Determination of antibacterial activity**

46 *Mycobacterium smegmatis* was grown in Middlebrook 7H9 medium supplemented with Middlebrook
47 ADC enrichment (Becton Dickinson), 0.5% v/v glycerol and 0.05% w/v Tween80. *E. coli* was cultured in
48 LB medium. *Staphylococcus aureus* was cultured in MH broth. We determined MICs against *M.*
49 *smegmatis* mc²155, *E. coli* JW5503 and *S. aureus* using a broth microdilution assays. The compound was
50 tested as a two-fold serial dilution at a starting concentration of 100 μM (final DMSO concentration of
51 2%). Growth was measured by OD and MIC₉₀ was recorded at the lowest concentration of compound
52 which inhibited growth by 90% compared to controls.

53

54 **Isolation of AN11527-resistant mutants**

55 *E. coli* JW5503 was plated on LB agar containing 4X and 8X MIC AN11527 at 8 x10⁸ to 2x10⁹ CFUs.
56 Single colonies were isolated after overnight incubation at 37°C and cultured in 5 ml LB for genomic
57 DNA isolation. Genomic DNA from resistant isolates was isolated and prepared for sequencing using the
58 Nextera XL library kit. Whole genome sequencing was carried out using 2 X 150 paired-end reads at the
59 Colorado State University whole genome sequencing facility. The *fabI* gene was PCR-amplified using

60 primers 5'- ATGGGTTTTCTTTCCGGTAAGCGCATTC -3' and 5'-
61 TTATTTTCAGTTTCGAGTTCGTTCA -3' and sequenced.

62

63 **Cloning and purification of *E. coli* FabI**

64 *E. coli* *FabI* gene was PCR-amplified using primer pair 5'-CATATG
65 ATGGGTTTTCTTTCCGGTAAGCGCAC-3 and 5'- GATCC TTATTTTCAGTTTCGAGTTCGTTTC-3
66 primers. The PCR product was cloned in to pET15(b) using sites NdeI and BamHI to obtain the plasmid
67 pET15b-FabI expressing FabI with an N-terminal His tag. FabI was expressed in BL21 (DE3) cells as
68 follows: cells were grown to an OD of 0.4 to 0.6, 1 mM IPTG was added and protein was purified from
69 the soluble fraction using a Ni- NTA column with 50 mM HEPES pH 8.0, 500 mM NaCl, 5% glycerol, 1
70 mM EDTA, 1 mM DTT. The purified protein was concentrated and stored in buffer containing 50mM
71 HEPES pH 8.0, 500 mM NaCl, 50% glycerol, 5 mM DTT. FabI A197G was constructed by site directed
72 mutagenesis using primers (5' CCGTACTCTGGCGGGATCCGGTATCAAAG 3') and (5'
73 CTTTGATACCGGATCCCGCCAGAGTACGG 3').

74

75 **Thermal shift assays**

76 We determined protein melting temperatures using the Prometheus NT.48 instrument (NanoTemper
77 Technologies). Purified FabI was diluted to a concentration of 25 μ M in 50 nM HEPES, 200mM NaCl.
78 Compound was added from 1.56 to 200 μ M; NADH and NAD⁺ were used at 250 μ M. The reaction
79 mixture was incubated at 25 C for 10 mins, 10 μ L sample was loaded into the capillaries and placed on
80 the sample holder. A temperature gradient from 20 °C to 80 °C at 0.5 or 1°C per min was applied.
81 Intrinsic protein fluorescence at 330 and 350 nm was recorded and the T_m was calculated using Nano
82 Temper Technologies software.

83

84 **Results and Discussion**

85 **The benzoxaborole AN11527 is active against *E. coli***

86 We determined the activity of a novel benzoxaborole against *M. smegmatis*, *S. aureus* and *E. coli*. We
87 used a *tolC* mutant strain of *E. coli* (JW5503). Although the compound showed good potency against *M.*
88 *tuberculosis* (2), it had no activity against the non-pathogenic organism *M. smegmatis* (MIC >200 µM).
89 There was no activity against the Gram positive species, *S. aureus* (MIC >200 µM). However,
90 surprisingly there was good activity against the Gram negative organism, *E. coli* with an MIC of 6.25 µM.

91

92 Since *E. coli* was sensitive, we isolated resistant mutants in order to identify the target or mechanism of
93 resistance. We plated 10⁸-10⁹ CFU on agar plates with 25 or 50 µM (4X and 8X MIC) compound and
94 isolated resistant mutants. We confirmed that strains were resistant by streaking onto solid medium with
95 25 µM AN11527. Resistance was further confirmed in liquid broth and all mutant strains exhibited high-
96 level resistance with > 32-fold shift in MIC (Table 1).

97

98 We conducted whole genome sequencing on two resistant-mutants and the wild-type strain with more
99 than 96% coverage and we identified mutations in *fabI*. Previous work has demonstrated that similar
100 compounds target mycobacterial InhA (4) an ortholog of FabI, and diazaborines are known to inhibit
101 FabI (5). FabI and InhA are involved in the synthesis of fatty acids, although InhA is a enoyl acyl carrier
102 protein reductase involved in the synthesis of mycolic acids which are specific to mycobacteria (6). Thus,
103 it seemed possible that FabI is the target in *E. coli*. We selected 21 AN11527-resistant strains and
104 sequenced *fabI* (Table 1). All of the strains had SNPs in *fabI* covering 9 different amino acid residues
105 with 12 different mutations (11 SNPs and 1 deletion) (Table 1).

106

107 The crystal structure of FabI in *E. coli* has been determined (9,12). We mapped the amino acid residues
108 from our resistant isolates onto the three-dimensional structure. The mutations form a cluster large
109 enough to encompass a molecule of AN11527 and are located around the active center site (Figure 1).
110 Several of the residues lie close to the NADH/NAD⁺ binding site (Figure 2) and are involved in the co-
111 factor binding. The binding pocket for AN11527 overlaps with other FabI inhibitors including a 4-
112 hydroxy-2-pyridine (NITD-916), isoniazid, and triclosan (7–9) (Figure 3). Therefore, we determined
113 whether the mutations also conferred resistance to triclosan. We observed a range of resistance for the
114 different mutations, with SNPs in I92, I192, F203 all conferring >4-fold resistance (Table 1). The I92L
115 allele conferred high level resistance (>80-fold), whereas mutations in F203 had varying resistance from
116 4-16-fold. Interestingly, the A116T allele conferred susceptibility to triclosan.

117

118 **Mycobacterial InhA inhibitors are active against *E. coli***

119 Previous work suggested that the 4-hydroxy-2-pyridine compound NITD-916 is active against *M.*
120 *tuberculosis*, but not *E. coli* (7). Since the benzoxaborole was active against *E. coli* and there is good
121 structural similarity between FabI and InhA, we tested it for activity against the TolC mutant strain. We
122 found that NITD-916 had good activity (MIC = 6.25 μM; Table 1) and thus its lack of activity is likely
123 due to efflux and lack of access to the target, as has been demonstrated for other FabI inhibitors in *E. coli*
124 (10). We tested our mutant isolates for cross-resistance to NITD-916; only two mutants showed low level
125 resistance (A21V and I192F) (Table 1). Both of these residues interact with the co-factor and this may
126 have an indirect effect on AN11527 and NITD-916 binding. However, several mutants were
127 hypersensitive (A197G, F203V and F203S). The equivalent of FabI F203 in *M. tuberculosis* is I215
128 which is involved in NITD-916 binding. However, in *E. coli* the InhA_{F203} mutant strain did not exhibit

129 cross-resistance or hypersensitivity to NITD-916 (Figure 4). Thus, even though the binding pocket of
130 NITD-916 and AN11527 overlaps, the lack of cross-resistance suggests differences in binding.

131

132 **AN11527 binding to FabI is co-factor dependent**

133 FabI is a fatty acid reductase which uses cellular NADH as a co-factor to reduce the enoyl carbon of fatty
134 acids (8). FabI inhibitors can be divided in two groups based on whether their binding is co-factor
135 dependent or independent. Depending upon the mechanism of interaction bacterial FabI inhibitors are
136 categorized in two groups, one that requires a co-factor (NAD⁺/NADH) to bind and another class which
137 binds directly (11).

138

139 We determined whether benzoxaborole binding was co-factor dependent using thermal shift assays.
140 NAD⁺-dependent binding of triclosan resulted in a large thermal shift (Table 2). No changes in T_m were
141 observed when incubated with AN11527 alone or AN11527 plus NADH. However, AN11527 in the
142 presence of NAD⁺ resulted in a shift. We confirmed this shift was dose-dependent (Table 3). We also
143 tested the FabI_{A197G} allele for binding. As expected, no thermal shift was seen in the presence of AN11527
144 even in the presence of NAD⁺, confirming loss of binding. Triclosan was still able to bind to the mutant
145 protein in the presence of NAD⁺ as expected from the lack of resistance of the strain. These data further
146 support that FabI is the target of AN11527 in *E. coli*.

147

148 **Conclusion**

149 FabI is an essential enzyme in many bacterial species, as it catalyzes a key step in the biosynthesis of fatty
150 acid pathway as part of the FAS II complex. It is interesting to note that although the substrates and
151 products for FabI and the mycobacterial ortholog InhA are different, a number of inhibitors are active

152 against both enzymes (11). A wide range of FabI/InhA inhibitors have been identified including the
153 frontline tuberculosis drug isoniazid and the antibacterial agent triclosan, as well as series under
154 development such as the 4-hydroxy-2-pyridine compound NITD-916. We demonstrate that a
155 benzoxaborole compound and NITD-916 are both active against the *E. coli* target and that resistance
156 maps to FabI. We demonstrate that AN11527 binds to InhA in a co-factor dependent manner which is
157 abrogated in mutant proteins.

158

159 **References**

- 160 1. O'Neil J. 2014. Review on antibiotic resistance. Antimicrobial Resistance : Tackling a crisis for
161 the health and wealth of nations Health and Wealth Nations.
- 162 2. Patel N, O'Malley T, Zhang YK, Xia Y, Sunde B, Flint L, Korkegian A, Ioerger TR, Sacchettini J,
163 Alley MRK, Parish T. 2017. A novel 6-benzyl ether benzoxaborole is active against
164 mycobacterium tuberculosis in vitro. Antimicrob Agents Chemother 61.
- 165 3. Low KL, Shui G, Natter K, Yeo WK, Kohlwein SD, Dick T, Rao SPS, Wenk MR. 2010. Lipid
166 droplet-associated proteins are involved in the biosynthesis and hydrolysis of triacylglycerol in
167 *Mycobacterium bovis* bacillus Calmette-Guérin. J Biol Chem 285:21662–21670.
- 168 4. Xia Y, Zhou Y, Carter DS, McNeil MB, Choi W, Halladay J, Berry PW, Mao W, Hernandez V,
169 O'Malley T, Korkegian A, Sunde B, Flint L, Woolhiser LK, Scherman MS, Gruppo V, Hastings
170 C, Robertson GT, Ioerger TR, Sacchettini J, Tonge PJ, Lenaerts AJ, Parish T, Alley MRK. 2018.
171 Discovery of a cofactor-independent inhibitor of *Mycobacterium tuberculosis* InhA. Life Sci
172 Alliance 1:e201800025.
- 173 5. Jordan CA, Sandoval BA, Seroby M V., Gilling DH, Groziak MP, Xu HH, Vey JL. 2015.
174 Crystallographic insights into the structure-activity relationships of diazaborine enoyl-ACP

- 175 reductase inhibitors. *Acta Crystallogr Sect Struct Biol Commun* 71:1521–1530.
- 176 6. Dessen A, Quémard A, Blanchard JS, Jacobs WR, Sacchettini JC. 1995. Crystal structure and
177 function of the isoniazid target of *Mycobacterium tuberculosis*. *Science* (80-) 267:1638–1641.
- 178 7. Manjunatha UH, Rao SPS, Kondreddi RR, Noble CG, Camacho LR, Tan BH, Ng SH, Ng PS, Ma
179 NL, Lakshminarayana SB, Herve M, Barnes SW, Yu W, Kuhen K, Blasco F, Beer D, Walker JR,
180 Tonge PJ, Glynn R, Smith PW, Diagana TT. 2015. Direct inhibitors of InhA are active against
181 *Mycobacterium tuberculosis*. *Sci Transl Med* 7:269ra3.
- 182 8. Rafi S, Novichenok P, Kolappan S, Zhang X, Stratton CF, Rawat R, Kisker C, Simmerling C,
183 Tonge PJ. 2006. Structure of acyl carrier protein bound to FabI, the FASII enoyl reductase from
184 *Escherichia coli*. *J Biol Chem* 281:39285–39293.
- 185 9. Sivaraman S, Zwahlen J, Bell AF, Hedstrom L, Tonge PJ. 2003. Structure-activity studies of the
186 inhibition of FabI, the enoyl reductase from *Escherichia coli*, by Triclosan: Kinetic analysis of
187 mutant FabIs. *Biochemistry* 42:4406–4413.
- 188 10. Parker EN, Drown BS, Geddes EJ, Lee HY, Ismail N, Lau GW, Hergenrother PJ. 2020.
189 Implementation of permeation rules leads to a FabI inhibitor with activity against Gram-negative
190 pathogens. *Nat Microbiol* 5:67–75.
- 191 11. Lu H, Tonge PJ. 2008. Inhibitors of FabI, an enzyme drug target in the bacterial fatty acid
192 biosynthesis pathway. *Acc Chem Res* 41:11–20.
- 193 12. Qiu X, Janson CA, Court RI, Smyth MG, Payne DJ, Abdel-Meguid SS. Molecular basis for
194 triclosan activity involves a flipping loop in the active site. *Protein Sci.* 1999 Nov;8(11):2529-32.
195 doi: 10.1110/ps.8.11.2529. PMID: 10595560; PMCID: PMC2144207.

196

197

198 **Tables**

199 **Table 1. Characterization of resistant mutants.**

FabI allele	Number of isolates	AN11527		NITD-916		Triclosan	
		MIC (μ M)	Fold-change	MIC ₉₀ (μ M)	Fold-change	MIC ₉₀ (μ M)	Fold-change
wild-type		6.25	n/a	6.3	n/a	0.16	n/a
A21V	1	>200	>32	50	4	0.062	0.4
I92L	1	>200	>32	12.5	2	12.5	80
G93S	4	>200	>32	6.3	1	nt	nt
A116T	1	>200	>32	6.3	1	0.0097	0.06
P191S	1	>200	>32	3.1	0.50	0.31	2
I192F	1	>200	>32	50	4.0	0.63	4
A197G	2	>200	>32	1.6	0.24	0.16	1
F203L	6	>200	>32	6.3	1.0	0.63	4
F203V	1	>200	>32	0.78	0.12	2.5	16
F203C	1	>200	>32	3.1	0.50	0.63	4
F203S	1	>200	>32	0.39	0.12	1.3	8
V213del	1	>200	>32	nt	nt	nt	nt

200

201 Minimum inhibitory concentrations (MIC) were determined in liquid medium against *E. coli* JW5503 and

202 AN11527-resistant *E. coli* JW5503. Data are from two independent runs.

203

204

205

206 **Table 2. Interaction of FabI with AN11527**

Allele	Molecule	Concentration	NAD ⁺	T _m	Shift
FabI_{wt}	None		-	52.1	
	AN11527		-	52.1	
	None		+	52.1	
	AN11527		+	56	3.9
	Triclosan		+	71.9	19.8
FabI_{A197G}	None		-	51.4	
	AN11527		-	51.2	
	None		+	51.3	
	AN11527		+	52.2	0.9
	Triclosan		+	65	13.7

207

208 FabI melting temperatures were measured by nanoDSF. Each sample contained 25 nM FabI plus
209 compound at 200 μ M and NAD⁺ at 250 μ M, where stated. The inflection point in $^{\circ}$ C was recorded as the
210 melting temperature; shifts are the difference in T_m. Data are representative of two independent
211 experiments.

212

213

Allele	Molecule	Concentration	NAD ⁺	T _m	Shift
FabI_{wt}	AN11527	200 μM	+	56	3.9
	AN11527	50 μM	+	54.9	2.8
	AN11527	12.5 μM	+	53	0.9
	AN11527	3.2 μM	+	52.1	0

214

215 **Table 3. Dose-dependent thermal shift of FabI with AN11527**

216 FabI melting temperatures were measured by nanoDSF. Each sample contained 25 μM FabI plus
217 compound and 250 μM NAD⁺. The inflection point in °C was recorded as the melting temperature; shifts
218 are the difference in T_m. Data are representative of two independent experiments.

219

220

221

222

223

224

225

226

227

228

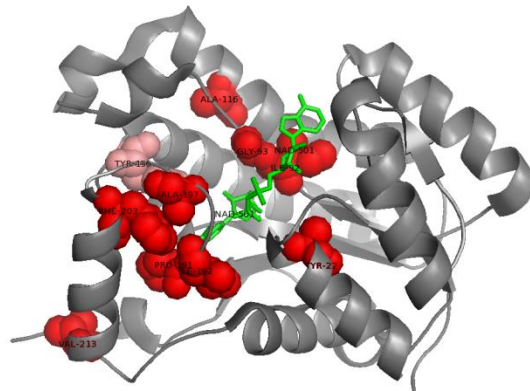
229

230 **Figure 1. Crystal structure of FabI (1D8A).**

231 (A) Residues that confer resistance to AN11527 are shown in red and NAD⁺ in green. The catalytic
232 residue Y156 is in pink. Residues that confer resistance to AN11527 are highlighted in red and are located
233 around the catalytic residue, the active center and close to the NAD⁺ binding site.

234

235



236

237

238

239

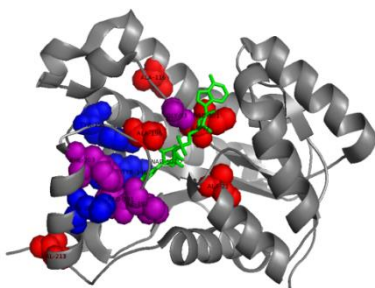
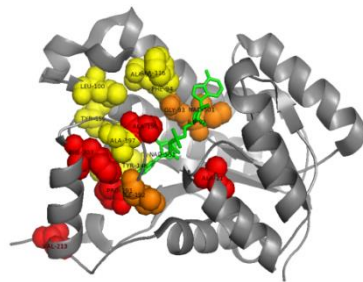
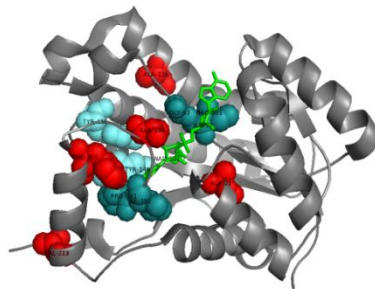
240 **Figure 2: Comparison of the binding pockets for FabI inhibitors.**

241 The proposed binding pocket of each inhibitor occupies the same general area around the active center
242 site and is close to the NAD⁺ binding location (FabI crystal structure 1D8A). Residues that confer
243 resistance to AN11527 are in red. NAD⁺ is shown bound. For isoniazid and NITD-916 interacting
244 residues are selected based on FabI and InhA homology. (A) Residues that confer resistance to isoniazid
245 are light green; residues that confer resistance to both isoniazid and AN11527 are in dark green. (B)
246 Residues that confer resistance to triclosan are light yellow; residues that confers resistance to both
247 isoniazid and AN11527 are dark orange. (C) Residues that confer resistance to NITD-916 are blue;
248 residues that confer resistance to both NITD-916 and AN11527 are purple.

249
250
251
252
253
254
255
256

257

258
259
260
261
262
263



264 **Figure 3: Location of FabI F203 and InhA I215**

265 Superimposition of FabI and InhA structures; *E. coli* FabI with triclosan in grey and *M. tuberculosis* InhA
266 with NITD-916 in cyan. In yellow and orange are the catalytic residue Y156 and in red and purple are the
267 residue FabI F203 and InhA I215 respectively.

268

269

270

271

272

273

274

275

276

277

278

279

280

281

282

